

209/2

# Directional Wave Measurements and Modelling

N.M. ANAND, B.U. NAYAK, S.S. BHAT AND V. SANIL KUMAR

Ocean Engineering Division,

National Institute of Oceanography, Goa-403 004, India

## ABSTRACT

Some of the results obtained from analysis of the monsoon directional wave data measured over 4 years in shallow waters off the west coast of India are presented. The directional spectrum computed from the time series data seems to indicate the predominant direction of waves as from SW to W as also the presence of sea and swell states. Measured one-dimensional spectra seem to show a possible narrowing tendency with increase in  $Uc/Cp$ . Two-dimensional spectra modelled as a product of measured one-dimensional spectra and  $\text{sech}^2(\beta\theta)$  spreading function seem to provide a better estimate of the directional energy distribution for the monsoon conditions. While non-linear wave-wave interaction seems to be the major governing factor in the directional spread of energy at and around the peak, direct wind input seems to influence the higher frequency part of the spectrum beyond the peak frequency.

## INTRODUCTION

A one-dimensional or all-directional spectrum is a representation of surface wave energy density function,  $S(f)$ , against various wave frequencies,  $f$ . On the other hand, a directional wave spectrum,  $S(f, \theta)$ , is one in which the above representation is classified into various directions of wave propagation,  $\theta$ . As the directional spectrum gives more complete and detailed information on wave behaviour, it is becoming an essential input in various ocean engineering studies like analysis and design of offshore structures, wave prediction, wave propagation problems, coastal process, etc. [2, 5, 6, 9, 11-13].

Although need for directional representation of ocean wave environment to provide the above information was felt two decades ago, only recently instruments have been designed to measure such information. Primarily, two types of measuring methods can be cited apart from remote sensing method, namely, array type and point measurement type. In the array type, simultaneously measured heave values are recorded, whereas in point type, a set of heaves and two perpendicular slopes are collected using a wave surface following buoy. Since maintaining and

operating a point type measuring system is simpler in high seas, it has commercially become popular and theories related to time series analysis of data so collected have been much reviewed and improved. This theory is aimed at obtaining frequency dependent directional information on wave activity leading to two-dimensional spectra. However, a strong wave frequency dependent nature of directional behaviour of observed sea depicted in terms of spreading function has not been modelled adequately and has often been over-simplified for design application.

This paper presents some of the important results obtained from the analysis of directional wave data measured at 16 m water depth off the west coast of India (Fig. 1). The directional spectrum computed from the time series data on the heave, pitch-roll buoy clearly indicates the presence of the sea and the swell environment.

Based on the wind data for almost one year duration, one-dimensional energy spectral characteristics at the measurement location have been discussed. In the past, attempts have been made to parameterize the spreading function in various ways. Some workers [6,9,11,14] have proposed spreading functions to estimate the direction spread of wave energy. An attempt has been made to model the directional energy distribution based on the measured directional wave data and

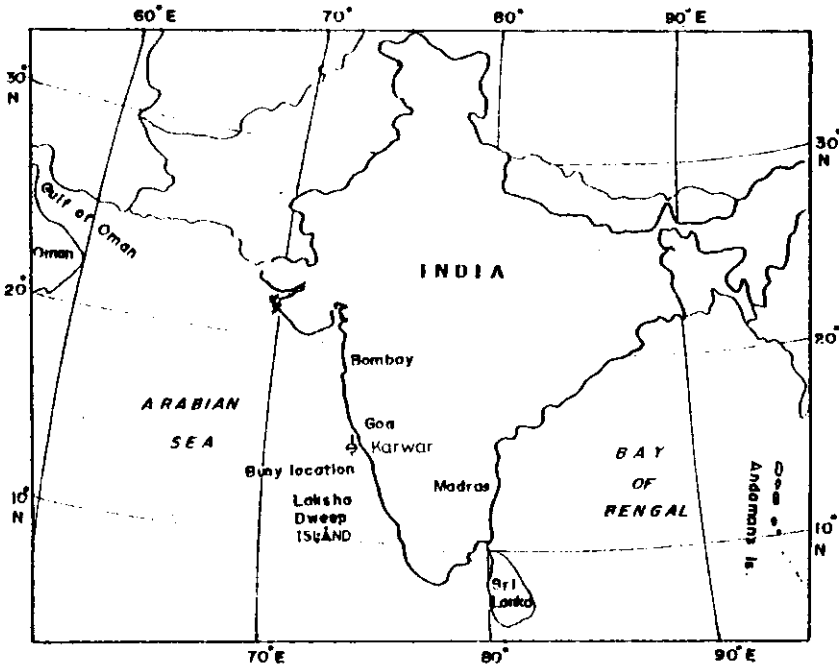


Fig. 1 — Location map

using some of the important directional spread models. To evaluate the spectral shape, it would be beneficial to study the influence of non-linear wave-wave interaction ( $f/fp$ ) and the direct wind input ( $Uc/Cp$ ) in the energy-contained region of the spectra. The concept of half-height width proposed by Donelan *et al.* [6] has been adopted in the present study to evaluate the above.

## DIRECTIONAL WAVE SPECTRUM

### Theory

Sea surface elevation can be best represented by visualising the energy contribution to the spectrum from waves having different frequencies and directions. Pitch-roll buoy measures heave and two horizontally perpendicular slope signals, allowing estimation of  $S(f)$ ,  $A_1$ ,  $B_1$  and  $A_2$ ,  $B_2$  only through cross-spectral calculations. The directional information is contained in these harmonic coefficients. These are first converted into harmonic amplitude  $m_1$ , and then mean direction  $\theta_0(f)$ , the spread  $\sigma_0(f)$  to compute 's' parameter. The standard method of analysis is described by Longuet-Higgins *et al.* [9] and Cartwright [3]. It requires the 2-D spectrum  $S(f, \theta)$  to be expressed as the product of its non-directional frequency spectrum  $S(f)$ , and its angular distribution  $D(f, \theta)$ , at each frequency  $f$ .

$$S(f, \theta) = s(f) * D(f, \theta) \quad \dots(1)$$

$$\text{where } \int_{-\pi}^{\pi} D(f, \theta) = 1 \quad \dots(2)$$

The distribution is considered as the sum of normalised angular harmonics at each frequency.

$$D(f, \theta) = 1/\pi (1/2) + \Sigma [A_n(f) \cos(n\theta) + B_n(f) \sin(n\theta)] \quad \dots(3)$$

$$m_1^2 = A_1^2 + B_1^2 \quad \dots(4)$$

$$\theta_0(f) = \text{arc tan}(B_1/A_1) \quad \dots(5)$$

$$\sigma_0(f) = [2(1-m_1)]^{1/2} \quad \dots(6)$$

$$s_1 = m_1/(1-m_1) \quad \dots(7)$$

### Theoretical spreading functions

Basically, two techniques of analyses are available. The first method involves reconstruction of the energy distribution and the second one involves identification of distribution characteristics at each frequency. Though the first method involves direct computation of harmonic components (Eq. 1) from the buoy signals, convolution of the distribution suggested by Longuet-Higgins *et al.* [9] arbitrarily broadens the estimations. The second method involves parametric

models which are based on *a priori* assumed shape of the directional energy distribution. Here, the number of independent shape parameters chosen should be less than 4, since only 4 Fourier coefficients are available [13]. Quite a few directional spreading functions are available for practical application. In the present study, the commonly used PNJ distribution and the  $\text{sech}^2(\beta\theta)$  type distribution proposed by Donelan *et al.* [6] have been considered.

### PNJ distribution

Pierson [14] proposed a cosine square type spreading function, which is defined as:

$$D(f, \theta) = (2/\pi) * \cos^{2s}(\theta - \theta_m) \text{ for } (\theta - \theta_m) < \pi/2$$

$$d(f, \theta) = 0 \quad \text{otherwise} \quad \dots(8)$$

where  $\theta_m$  is the mean wave direction.

### SECH<sup>2</sup>( $\beta\theta$ ) distribution

Donelan *et al.* [6], verifying the appropriateness of the  $\cos^{2s}(\theta)$  spreading function, found that it consistently errs by overestimating the wave energy at peak in the direction of wave propagation. They proposed an alternative function on the assumption that the distribution of wave energy in the direction transverse to the main direction is proportional to  $\text{sech}^2(\beta\theta)$ . Here,  $\beta$  determines the energy spread.

$$D(f, \theta) = (\beta/2) * \text{sech}^2\{\beta(\theta - \theta_m)\} \quad \dots(9)$$

$$\beta = 2.61 (f/f_p)^{1.3} \quad \text{for } 0.56 < f/f_p < 0.95$$

$$= 2.28 (f/f_p)^{-1.3} \quad \text{for } 0.95 < f/f_p < 1.60$$

$$= 1.24 \quad \text{otherwise.}$$

## MATERIALS AND METHODS

The Datawell WAVEC buoy (Fig. 2) was deployed in the Arabian Sea at a water depth of approximately 16 m and about 8 km away from the Karwar coast (Fig. 1). The buoy has a diameter of 2.5 m. A cylindrical can of 0.5 m diameter and 0.7 m height contains sensors, radio transmitter, other electronics and batteries. It protrudes through the bottom centre of the buoy to reduce current induced tilt of the buoy and to protect the main sensor from freezing. To prevent capsizing, a foam body is placed on the top of the hull. This foam body contains the radar reflector. The main sensor is a Hippy-120A, which measures the heave, pitch and roll motions of the buoy in a coordinate system relative to the buoy hull. The heave is determined by double integration of vertical acceleration of the platform. Pitch and roll angles are determined by measuring the fluxes of two oscillating magnetic fields through a pick-up coil on the platform. These fields are generated by two orthogonal coil systems in a fixed position relative to the buoy hull. A three-

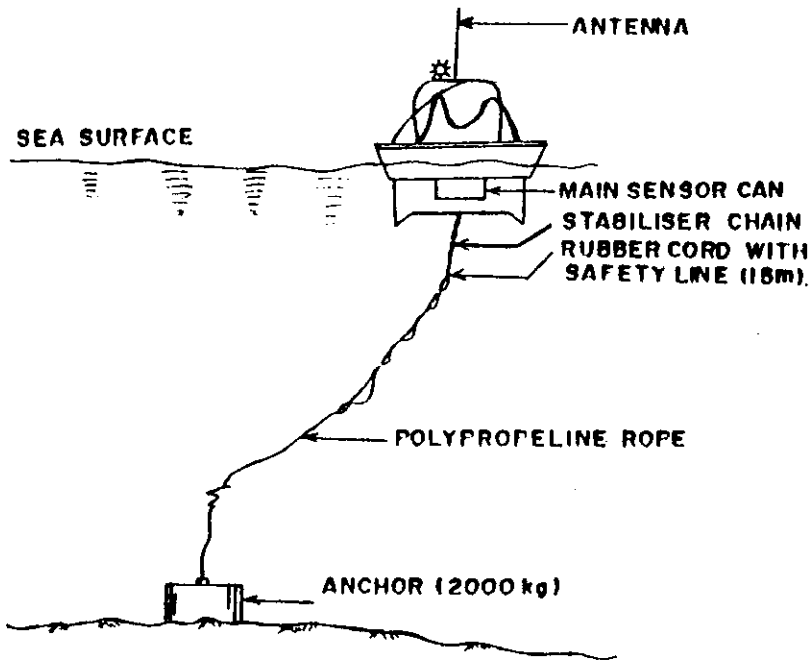


Fig. 2 — WAVEC buoy mooring system

dimensional fluxgate meter is used to measure the orientation of the hull fluxgate to magnetic north. Figure 2 shows the details of the buoy and the mooring system.

A 27 MHz radio link is used to send the data to a receiver which contains a microprocessor. This microprocessor performs real time analysis to determine directional wave characteristics. A desk-top computer is used to carry out on-line analysis and data storing. On-line analysis of six basic pitch-roll buoy signals is carried out for each record of 30 min to obtain information on the directional wave spectrum,  $S(f, \theta)$ , along with mean direction, r.m.s. spread values of wave energy and 's' parameter of the distribution at each 0.005Hz frequency. The time series is divided into nine blocks of each 200s and FFT analysis is carried out with sampling interval of 1.28s and cut-off frequency of 0.65Hz [1, 13].

## RESULTS AND DISCUSSION

Measured wave data pertaining to the monsoon period have been analysed for directional wave parameters and the results are presented in Table 1. In general, the value of  $H_s$  seems to exceed 2 m for about 60% of the time with directions

Table 1 — Joint Distribution

*Hs vs Tz*

Hs(m)	Tz(s)					Total
	2-4	4-6	6-8	8-10	10-12	
0.0-0.5	.	.	.	.	.	.
0.5-1.0	.	28	18	.	.	46
1.0-1.5	.	121	206	2	.	329
1.5-2.0	.	141	642	6	.	789
2.0-2.5	.	24	418	14	.	456
2.5-3.0	1	2	252	14	.	269
3.0-3.5	.	.	24	5	.	29
3.5-4.0	.	.	3	3	.	6
4.0-4.5	.	.	1	3	.	4
4.5-5.0	.	.	.	3	.	3
Total	1	316	1564	50	.	1931

*Hs vs Dm*

Hs(m)	Mean direction (deg)						Total
	120-150	150-180	180-210	210-240	240-270	270-300	
0.0-0.5	.	.	.	.	.	.	.
0.5-1.0	.	.	.	14	32	.	46
1.0-1.5	1	.	3	95	230	.	329
1.5-2.0	.	.	1	42	744	2	789
2.0-2.5	.	.	.	8	448	.	456
2.5-3.0	.	.	.	1	268	.	269
3.0-3.5	.	.	.	.	.	29	.
3.5-4.0	.	.	.	1	5	.	6
4.0-4.5	.	.	.	.	4	.	4
4.5-5.0	.	.	.	.	3	.	3
Total	1	.	4	161	1763	2	1931

between SW and W and periods  $T_z$  between 6 to 8 sec. Examples of premonsoon and monsoon spectra shown in Fig.3 reveal the presence of sea and swell environment.

In the general case of winds that are variable in speed and direction, a description of the parameters of the spectrum in terms of local conditions would be valuable. Hence, it is meaningful to relate the spectral parameters to  $Uc/Cp$  values, where  $Uc$  is the component of 10 m wind speed in the direction of the waves and  $Cp$  is the celerity of the waves with peak frequency. In all, 7 ranges of  $Uc/Cp$  values, viz, 0.0-0.1, 0.1-0.2, 0.2-0.3 ..... and 0.6-0.7 were available from the measured wave and the wind data (Table 2). Figure 4 shows measured one-dimensional spectra pertaining to the above ranges of  $Uc/Cp$  values. In general, even though at all ranges of  $Uc/Cp$ , spectra show a well defined peak, low energy secondary peaks seem to be present at higher frequencies beyond the peak frequency showing the presence of sea and swell states. These secondary peaks seem to grow bigger as the  $Uc/Cp$  value increases showing the influence of direct wind input in the growth of higher frequency part of the spectra. It appears that there is a pronounced narrowing of the spectra at and around the peak with increasing  $Uc/Cp$  values.

Figures 5 and 6 show the 2-D spectra derived as a product of the measured non-directional spectra pertaining to the 7 ranges of  $Uc/Cp$  values and the two theoretical directional energy spread functions considered. The polar spectra seem to be predominantly unimodal and tend to be symmetrical about their peaks. However, the low energy secondary modes at higher frequencies beyond the peak frequency could also be seen. As the data pertain to the monsoon period, local wind influence as discussed earlier seems to be the possible cause. While modelling the energy spread, mean wind direction is taken as the mean wave direction. Another noticeable aspect is the directional broadening of the spectral contours

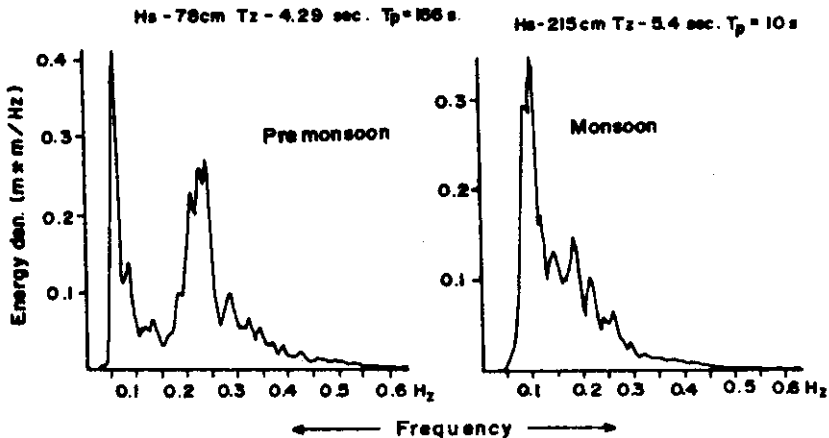


Fig. 3 — Typical premonsoon and monsoon spectra

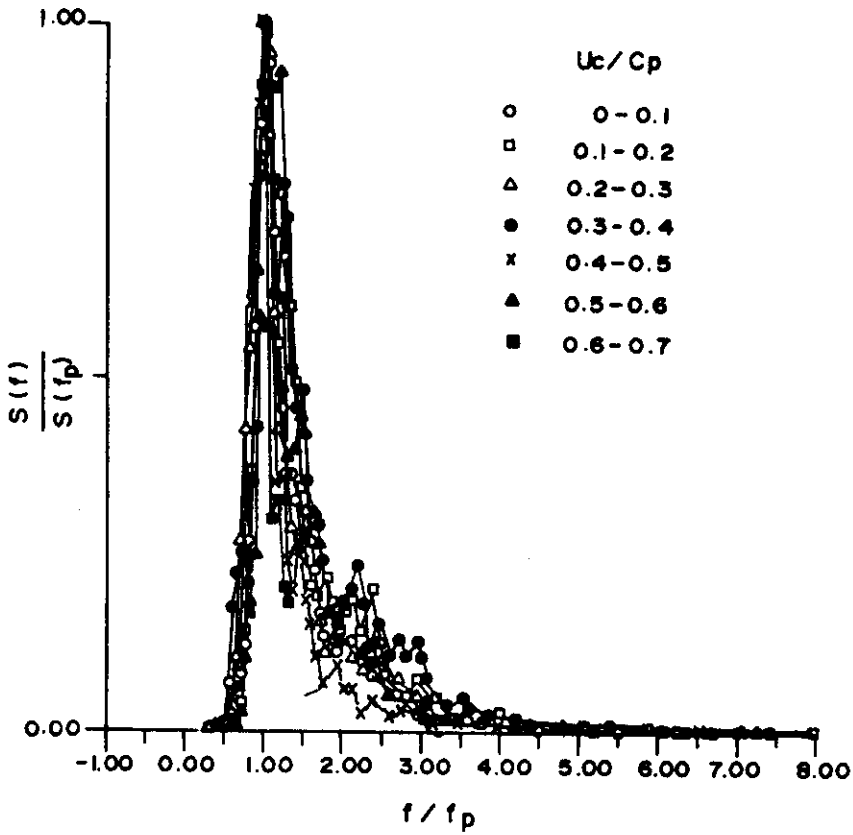


Fig. 4 — Normalised frequency spectra grouped into classes by  $U_o/C_p$

Table 2 — Directional Wave Characteristics

$H_s$	$E_{max}$	$T_z$	$T_p$	$U$	$U_{dir}$	$U_o/C_p$
2.83	9.99	7.66	11.70	1.94	197.0	0.0-0.1
2.85	9.53	7.42	13.30	3.51	241.0	0.1-0.2
1.81	3.74	7.32	11.70	2.98	240.0	0.2-0.3
2.51	6.13	6.96	12.50	7.01	223.0	0.3-0.4
2.55	8.96	7.68	11.10	5.15	214.1	0.4-0.5
3.08	11.80	7.53	12.50	6.34	203.8	0.5-0.6
2.33	7.46	6.53	10.50	8.32	210.5	0.6-0.7



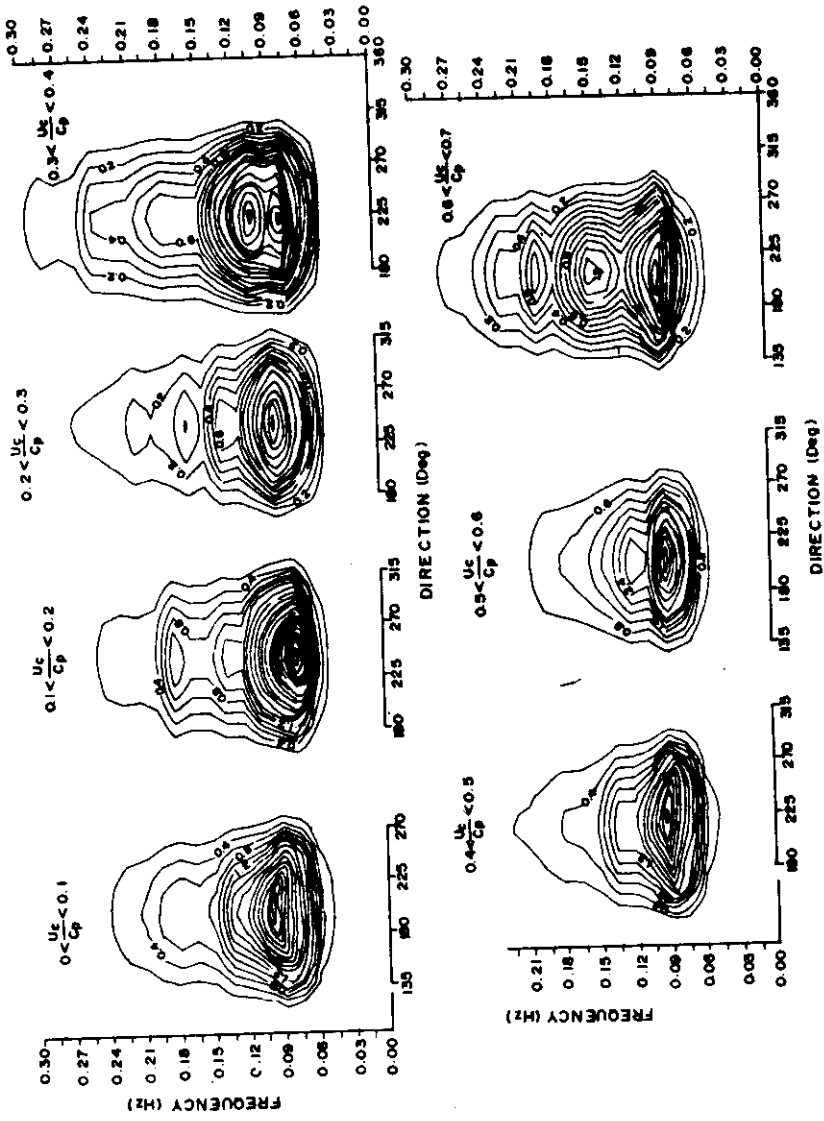


Fig. 5 — Polar plots of PNJ distribution

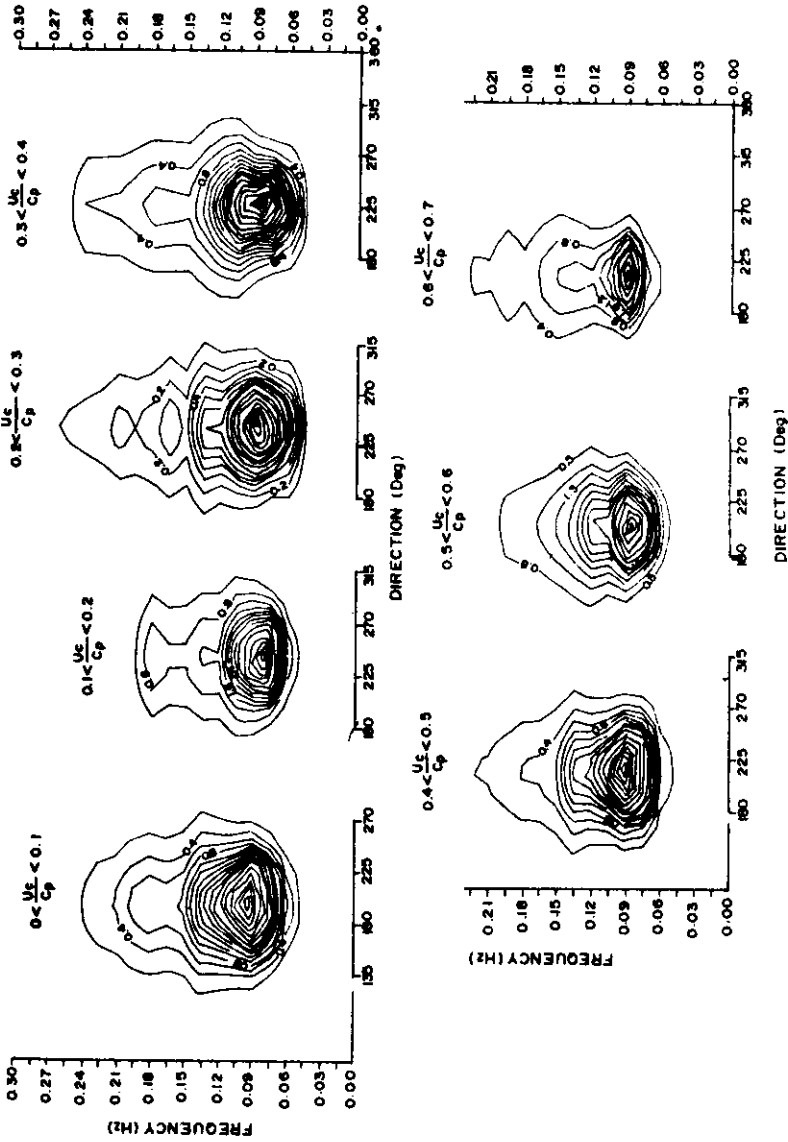


Fig. 6 — Polar plots of  $\text{sech}^2(\beta\theta)$  distribution

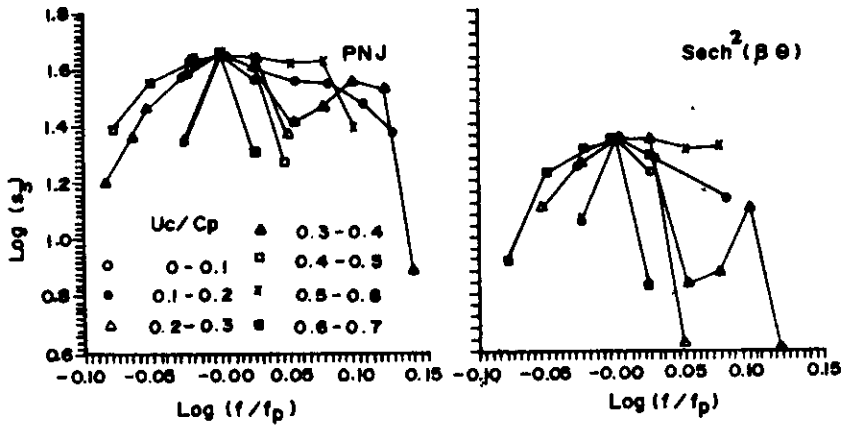


Fig. 7 — The  $s$  parameter calculated from the half-height of polar distributions

with increasing frequency above the peak. The 2-D spectra modelled, using the  $\text{Sech}^2(\beta\theta)$  spreading function, seem to show more clustering of contours and smaller angular spread of wave energy around the peak compared to that from the  $\cos^{2s}(\theta)$  spreading function. Also, the range of angular spread obtained from  $\text{Sech}^2(\beta\theta)$  spreading function is more or less of similar range compared to that computed from the measured data. This seems to suggest that  $\text{sech}^2(\beta\theta)$  describes the directional energy distribution better compared to the  $\cos^{2s}(\theta)$  spreading function in the present case in the energy containing region of the spectra.

To study the directional spread in the energy containing region of the spectra, widths at half height,  $s_3$ , of the polar plot for various ranges of  $U_c/C_p$  values have been evaluated. Figure 7 shows plots of  $\log(S_3)$  vs  $\log(f/f_p)$  for the two-directional spread functions considered. One common feature is that the spread function at and near the peak (5% of  $f_p$ ) seems to depend only on  $f/f_p$ . This seems to suggest that the spreading of wave energy at and near the peak is more governed by non-linear wave-wave interaction process than by the direct wind input, which confirms with the results of Hasselmann *et al.* [7] and Donelan *et al.* [6].

## CONCLUSION

Based on the analysis of directional wave data pertaining to monsoon season, the following conclusions have been arrived at:

- i)  $H_s$  values seem to exceed 2 m for about 60% of the time with directions between SW to W and period  $T_z$  between 6 to 8 sec.
- ii) Spectra show the presence of sea and swell states.

- iii) Increase in  $Uc/C_p$  values seems to influence the wave growth more at higher frequencies (rear face) of the spectra than at lower frequencies (forward face).
- iv) The spreading function  $\text{sech}^2(\beta\theta)$  proposed by Donelan *et al.* [6] seems to model the directional energy distribution better compared to the PNJ spreading function. Further studies are needed to justify the selection of mean wind direction as the mean wave direction, as this need not be true at all locations.

### ACKNOWLEDGEMENT

The authors express their deep gratitude to the Director, for support and encouragement and to the divisional colleagues for their help during the wave data collection and analysis programme.

### REFERENCES

1. Bhat, S.S., S. Mandal and B.U. Nayak. 1989. Directional wave spectra of Bombay Coast. *25th Annual Convention on Indian Geophysics Union*, Hyderabad, India.
2. Borgman, L.E. 1969. Directional models for design use, *Proceedings of Offshore Technology Conference*, Paper No. 1069: 721-746.
3. Cartwright, D.E. 1963. The use of Directional spectra in studying the outputs of a recorder on movstanding ship. *Proceedings of Conference on Ocean Wave Spectra*, Easton MD, Prentice Hall: 203-219.
4. Deo, M.C. and S. Narasimhan. 1988. Generalised estimation of wave force spectra. *Journal of Waterways Port Coastal Ocean Engineering Division*, ASCE 114, Paper 22281.
5. Deo, M.C. 1989. Directional wave spectrum and its application. In: *Ocean Wave Studies and Application*, M. Baba and T.S. Shahul Hameed (Eds.), CESS, Trivandrum: 45-59.
6. Donelan, M.A., J. Hamilton and W.H. Hui. 1985. Directional wave spectra of wind generated waves. *Philos. Trans. R. Soc., London*. A.315: 509-562.
7. Hassellmann, D.E., M. Dunckel and J.A. Ewing. 1980. Directional wave spectra observed during JONSWAP 1973. *J. Phys. Oceanogr.* 10: 1264-1280.
8. Longuet-Higgins, M.S. 1962. The directional spectrum of ocean waves and processes of wave generation. *Philos. Trans. R. Soc. London*. A.265: 286-315.
9. Longuet-Higgins, M.S., D.E. Cartwright and N.D. Smith. 1963. Observation of directional spectrum of sea waves using motions of the floating buoy. *Ocean Wave Spectra National Academy of Science*, Easton: 111-136.
10. Malhotra, A.K. and J. Penzien. 1970. Non-deterministic analysis of offshore tower structures. *J. Engng. Mech.*, ASCE, 96: 985-1003.
11. Mitsuyasu, H.F. Tasai, T. Suhara, S. Muzuno, M. Ohkusu, T. Honda and K. Kikishi. 1975. Observations of the directional spectrum of ocean waves using a clover leaf buoy, *J. Phys. Oceanogr.* 5: 750-760.
12. Munk, W.H., G.R. Miller, F.E. Snodgrass and N.F. Barber. 1966. Directional recording of swells form distant storms. *Philos. Trans. R. Soc. London*. A. 255: 505-583.
13. Kuik, A.J., G. Vledder and Holthuisen. 1988. A method for routine analysis of heave-pitch-roll buoy wave data. *J. Geophys. Res.* 18: 1020-1034.
14. Pierson, W.J., G. Neumann and R.W. James. 1955. Practical methods for observing and forecasting ocean waves by means of wave spectra and statistics, Publ. No. 603, U.S. Naval Hydrographic Office.